



Original article

Dynamic of grassland vegetation degradation and its quantitative assessment in the northwest China

Wei Zhou^a, Chengcheng Gang^a, Liang Zhou^b, Yizhao Chen^a, Jianlong Li^{a,*}, Weimin Ju^c, Inakwu Odeh^d^a School of Life Science, Nanjing University, Hankou Road 22, Nanjing 210093, PR China^b School of Geographic and Oceanographic Sciences, Nanjing University, Nanjing 210093, PR China^c International Institute of Earth System Sciences, Nanjing University, Nanjing 210093, PR China^d Department of Environmental Sciences, Faculty of Agriculture and Environment, The University of Sydney, NSW 2006, Australia

ARTICLE INFO

Article history:

Received 18 April 2013

Accepted 22 December 2013

Available online 14 January 2014

Keywords:

Grassland degradation

Climate change

Human intervention

Grassland restoration

Tibetan plateau

ABSTRACT

Grasslands, one of the most widespread land cover types in China, are of great importance to natural environmental protection and socioeconomic development. An accurate quantitative assessment of the effects of inter-annual climate change and human activities on grassland productivity has great theoretical significance to understanding the driving mechanisms of grassland degradation. Net primary productivity (NPP) was selected as an indicator for analyzing grassland vegetation dynamics from 2001 to 2010. Potential NPP and the difference between potential NPP and actual NPP were used to represent the effects of climate and human factors, respectively, on grassland degradation. The results showed that 61.49% of grassland areas underwent degradation, whereas only 38.51% exhibited restoration. In addition, 65.75% of grassland degradation was caused by human activities whereas 19.94% was caused by inter-annual climate change. By contrast, 32.32% of grassland restoration was caused by human activities, whereas 56.56% was caused by climatic factors. Therefore, inter-annual climate change is the primary cause of grassland restoration, whereas human activities are the primary cause of grassland degradation. Grassland dynamics and the relative roles of climate and human factors in grassland degradation and restoration varied greatly across the five provinces studied. The contribution of human activities to grassland degradation was greater than that of climate change in all five provinces. Three outcomes were observed in grassland restoration: First, the contribution of climate to grassland restoration was greater than that of human activities, particularly in Qinghai, Inner Mongolia, and Xinjiang. Second, the contribution of human activities to grassland restoration was greater than that of climate in Gansu. Third, the two factors almost equally contributed to grassland restoration in Tibet. Therefore, the effectiveness of ecological restoration programs should be enhanced whenever climate change promotes grassland restoration.

© 2014 Elsevier Masson SAS. All rights reserved.

1. Introduction

Grasslands, one of the most common types of vegetation in the world, account for nearly 20% of the global land surface (Scurlock and Hall, 1998). Human food production and, to a lesser extent climate change, have profoundly influenced grasslands (Conant et al., 2001). China has 3.93 million km² of grasslands, which account for about 40% of China's total land area, and 6%–8% of the global total grassland area (Ni, 2002). However, nearly 90% of the grasslands in northern China have been degraded to some extent (Nan, 2005) at a rate of approximately 6700 km² each year (Yang,

2002) because of climate warming over the last 50 years (Chase et al., 2000), intensification of land use (Kang et al., 2007), population growth, and socioeconomic development. Land degradation has caused serious environmental and social problems, such as dust storms and decreased productivity and soil quality. To alleviate the multifaceted environmental degradation, the Chinese government has implemented several ecological restoration programs that have deeply affected the structure and function of grassland ecosystems (Wang et al., 2011).

Grassland conditions in China have changed considerably because of the implementation of restoration programs or the continual degradation of regions that have benefited little from government programs (Jiang et al., 2006). Such vegetation dynamics are caused by natural changes exacerbated by human activities (Xin, 2008).

* Corresponding author.

E-mail address: jianlongli@gmail.com (J. Li).

Although climate change and human activities are widely accepted as the main driving forces underlying grassland degradation, little research has been done to distinguish the individual effects of climate and human factors on grassland degradation. Therefore, the development of a quantitative method for assessing the relative effects of climate and human factors on grassland degradation is crucial for monitoring (Veron et al., 2006). Some studies have analyzed human-induced vegetation degradation using the rainfall use efficiency method (RUE) (Prince et al., 2004; Symeonakis and Drake, 2004). However, RUE is an oversimplified empirical indicator that provides unreliable results. Other studies have evaluated these relative roles using a localized statistical model of the vegetation–climate relationship (Evans and Geerken, 2004; Wang et al., 2012). Others have used vegetation dynamics to distinguish human-induced vegetation changes from climate change because vegetation dynamics is the most intuitive manifestation of land degradation (Wessels et al., 2007; Xu et al., 2010; Zhang et al., 2011). This assessment is accomplished by comparing the potential vegetation conditions with the actual conditions. Based on this concept, net primary productivity (NPP) is sensitive to both climate change and human effects (Schimel, 1995). Therefore, vegetation dynamics, as measured using NPP, have been used to distinguish the effects of climate change on ecosystems from those caused by human activities (Zheng et al., 2006; Wessels et al., 2008; Xu et al., 2010). Specifically, studies have used human appropriation of net primary production to measure the impact of human activities on regional and global ecosystems (Rojstaczer et al., 2001; Haberl et al., 2002).

In China, grasslands are mostly located in the northern temperate and Tibetan Plateau regions, which together account for 54% of the total land area and 78% of the total grassland in China (Chen and Wang, 2000). The region is sensitive to climate change and human intervention, as well as an ecologically fragile region, and is the origin of sandstorms in China (Wang et al., 2004a). The region is also home to about 40 million people.

In spite of the importance of this region, few studies have evaluated grassland degradation dynamics and assessed the causes of grassland degradation. Therefore, in this study, the forementioned regions are selected as the study area. Grassland degradation is related to issues such as declining productivity, biodiversity loss, land degradation, and declining ecosystem services (Turner et al., 2001). NPP, as a fundamental ecological variable, reflects grassland degradation and is easily calculated using remote sensing data. Therefore, we designed a quantitative method based on NPP. Actual NPP was used to evaluate the grassland degradation dynamics, the potential NPP, and the difference between potential NPP and actual NPP (LNPP) was used to assess the relative roles of climate and human activities in grassland degradation. Thus, the results of this study will provide recommendations for grassland resource management and sustainable development under the current situation of climate change and human intervention. The objectives of this study are as follows: 1) to evaluate the current status of grassland actual NPP; 2) to examine grassland vegetation degradation dynamics; 3) to assess separately the effects of inter-annual climate change and human activities on grassland degradation or restoration to determine the dominant factor; and 4) to establish a method for assessing the relative roles of climate and human factors in grassland degradation, and to provide a method for evaluating the effectiveness of ecological restoration programs.

2. Material and methods

2.1. Study area

The study region is located in northwest China and the Tibetan Plateau (26°05′–53°33′ N; 73°40′–135°02′ E), including the Inner

Mongolia Autonomous Region (IM), Xinjiang Uygur Autonomous Region, Tibet Autonomous Region, Qinghai, and Gansu. The grasslands in these five provinces account for 84.1% of the total grassland area in China according to the Global Land Cover 2000 dataset (GLC, 2003).

Northwest China is characterized by an arid to semiarid climate and large differences between daytime temperatures and nighttime temperatures. High mountains with high precipitation, such as Altai, Tianshan, Kunlun, and Qilian, block the atmospheric circulation and create vast desert basins in the rain shadow, such as Tarim, Junggar, and Qaidam (Shi et al., 2007). The IM has the largest grassland area in China, which includes meadows, plain grassland, and desert grassland (Fig. 1). The grasslands in Xinjiang Province consist of desert grasslands, plain grasslands, alpine and sub-alpine grasslands. The grassland in Gansu Province mainly consist of meadows near the north slope of the Qilian Mountains, slope grassland near the Loess Plateau, and alpine and sub-alpine grasslands near the edge of the Tibetan Plateau. This study area has undergone serious desertification and grassland degradation because of land use changes, overgrazing, and global warming.

The Tibetan Plateau is the highest contiguous area in the world, with a land area of approximately 1.4 million km² perched 4500 m above sea level (Huddleston et al., 2003). According to Chinese climate classification, the Tibetan Plateau has a “plateau climate” (Li, 1993), which is characterized by a subtropical to temperate mountain climate unique to the Qinghai–Tibet Plateau (Chen et al., 2006). The surface temperature at the Tibetan Plateau is relatively low because of its high altitude. However, the Tibetan Plateau has warmed since the mid-1950s. Precipitation in the Tibetan Plateau is relatively low and subject to extreme spatio-temporal variability (Ueno et al., 2001). The plateau is the source of numerous major rivers in southeastern and eastern Asia, including the Yellow River, the Yangtze River, the Mekong River, and the Salween River. The natural vegetation in the Tibetan Plateau varies greatly and consists of forests, grasslands, and shrubs, which are very vulnerable and sensitive to environmental changes and human activities. To date, the Tibetan Plateau approximately has 425,100 km² of degraded grasslands, 16% of which is severely degraded (Wang et al., 2006a).

2.2. Data sources and processing

2.2.1. Normalized difference vegetation index (NDVI) data

Moderate resolution imaging spectroradiometer (MODIS) data and geospatial meteorological data were selected as the input parameters for the Carnegie–Ames–Stanford Approach (CASA) model to calculate the NPP. A MODIS-derived 16-day composite, atmospherically corrected maximum vegetation indices (MOD13A1) with a spatial resolution of 500 m × 500 m were downloaded from the Earth Observing System data gateway (<http://ladsweb.nascom.nasa.gov/data/search.html>). A maximum-value compositing procedure was used to merge the 16-day NDVI data and generate monthly NDVI datasets. These MODIS–NDVI data were reprojected from the original integerized sinusoidal projection into an Albers equal area conical projection and WGS-84 datum using the MODIS reprojection tool, and were extracted through the vector boundary of the study area using ArcGIS V9.3 (ESRI, California, USA).

2.2.2. Meteorological data

Meteorological data for the study area from 2001 to 2010, including average monthly temperature and total precipitation for 245 stations and total solar radiation data for 45 stations in and around northwest China, were obtained from China Meteorological

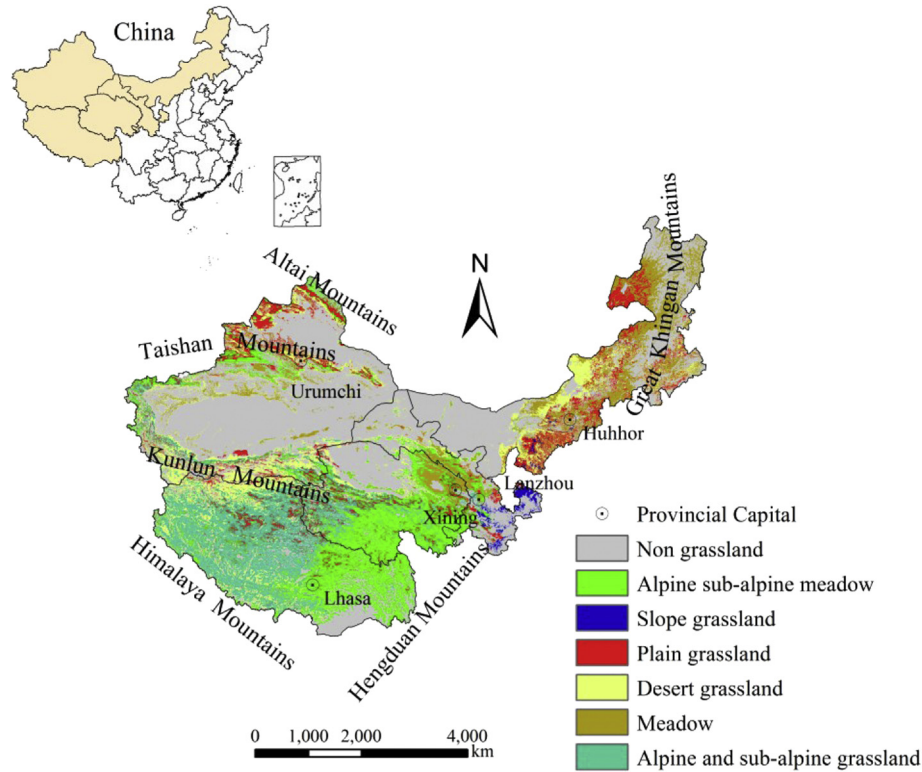


Fig. 1. Location of the study area showing the distribution of grassland types in the five provinces.

Data Sharing Service System. The ordinary Kriging interpolation method was used to interpolate meteorological data into a grid with $500 \text{ m} \times 500 \text{ m}$ spatial resolution. These monthly meteorological data were used to drive the CASA model.

The meteorological data required for the Thornthwaite memorial model are annual total precipitation and average temperature. These annual data were calculated from monthly temperature and precipitation. Raster meteorological data were also extracted using the vector boundary of the study area. The images with the same spatial resolution and coordinate system as those were used in the CASA model.

2.2.3. Field survey on NPP

We sampled 63 field sites across the study area in late July and April of 2009. At each site, we divided a sampling plot ($10 \text{ m} \times 10 \text{ m}$) into four quadrats ($5 \text{ m} \times 5 \text{ m}$), marked as S1, S2, S3, and S4. At each quadrat, we selected five small plots ($1 \text{ m} \times 1 \text{ m}$). To calculate the annual NPP, we determined the biomass at each site twice, once in early April in quadrats S1 and S3, and again at the end of August in quadrats S2 and S4. The annual grassland NPP was calculated as the difference between the maximum (measured at the end of July) and the minimum (measured in early April) biomass values. Biomass measurement was conducted as follows. All plants in each plot were harvested to determine aboveground biomass. Nine soil cores (8 cm in diameter) were used to collect samples at 10 cm intervals to determine belowground biomass. Root samples were immediately placed in a cooler and then transported to the laboratory. The samples were soaked in deionized water and cleaned of soil residue using a 0.5 mm mesh sieve. The biomass samples were oven dried at 65°C to a constant mass and weighed to the nearest 0.1 g. The biomass was subsequently converted into carbon content by using a conversion factor of 0.45 (Fang et al., 1996). At last, the increment of biomass carbon was the annual NPP.

2.3. Methods

2.3.1. Calculation of actual NPP based on CASA model

As an indicator for the overall condition of grassland degradation, NPP reflects the complex interactions between climate change and human activities (Hanafi and Jauffret, 2008). In the present study, actual NPP ($\text{g C m}^{-2} \text{ yr}^{-1}$) was used to assess grassland degradation dynamics. Actual NPP was calculated using the CASA model, a light use efficiency model based on the resource–balance theory (Potter et al., 1993; Field et al., 1995). In the CASA model, NPP is the product of absorbed photosynthetically active radiation (APAR) and light use efficiency (ϵ) (Potter et al., 1993). The basic principle of the model can be described as follows:

$$\text{NPP}(x, t) = \text{APAR}(x, t) \times \epsilon(x, t) \quad (1)$$

where x is the spatial location (pixel number), t is time, APAR represents the canopy-absorbed incident solar radiation integrated over a given time period (MJ m^{-2}), and $\epsilon(x, t)$ represents the actual light use efficiency (g C MJ^{-1}). APAR(x, t) and $\epsilon(x, t)$ are calculated using Eqs. (2) and (3):

$$\text{APAR}(x, t) = \text{SOL}(x, t) \times \text{FPAR}(x, t) \times 0.5 \quad (2)$$

where SOL(x, t) is the total solar radiation (MJ m^{-2}) of pixel x at time t , and FPAR(x, t) is the fraction of the photosynthetically active radiation absorbed by the vegetation. FPAR(x, t) can be determined using NDVI; 0.5 represents the proportion of the total solar radiation available for vegetation (wavelength range of $0.38 \mu\text{m}$ – $0.71 \mu\text{m}$). The algorithm for light use efficiency can be expressed as follows:

$$\epsilon(x, t) = T_{\epsilon 1}(x, t) \times T_{\epsilon 2}(x, t) \times W_{\epsilon}(x, t) \times \epsilon_{\text{max}} \quad (3)$$

where $T_{\varepsilon 1}(x, t)$ and $T_{\varepsilon 2}(x, t)$ denote the temperature stress coefficients, $T_{\varepsilon 1}(x, t)$ represents the influence of extreme temperature on light use efficiency (Field et al., 1995), $T_{\varepsilon 2}(x, t)$ reflects the decrease in light use efficiency when temperature deviates from the optimal level (Potter et al., 1993; Field et al., 1995), $W_{\varepsilon}(x, t)$ is the moisture stress coefficient that indicates the reduction in light use efficiency caused by the moisture factor, and ε_{\max} denotes the maximum light use efficiency under ideal conditions and can be set to different constant parameters for different vegetation types. The value of ε_{\max} for grassland is 0.542 in this study, in accordance with the study of Zhu et al. (2006). A more detailed description of this algorithm can be found in Yu et al. (2011).

2.3.2. Validation of the CASA model

The NPP determined from the field sampling in 2009 was compared with the simulated values to verify the estimation accuracy of the CASA model. Fig. 2 illustrates the correlation between the observed NPP and the estimated NPP ($R^2 = 0.635$, $P < 0.001$), which indicates that the model has a satisfactory estimation accuracy. However, the estimates were slightly higher than the actual field data. Nevertheless, this result does not alter the results of the NPP trend analysis.

2.3.3. Calculation of potential NPP based on the Thornthwaite memorial model

Although several models have been developed to estimate potential NPP, these models are based on different climatic factors. The Miami model (Lieth, 1975), the first widely used model, is derived from the correlations between measured NPP and the corresponding temperature and precipitation data. The Thornthwaite memorial model was established according to the data used in the Miami model, but was modified to include Thornthwaite's potential evaporation model (Lieth and Box, 1972). In this study, potential NPP was simulated using the Thornthwaite memorial model. The model can be expressed as follows:

$$NPP = 3000 \left[1 - e^{-0.0009695(v-20)} \right] \tag{4}$$

where NPP is the annual total NPP and v is the annual actual evapotranspiration (mm). The calculated equations are expressed as follows:

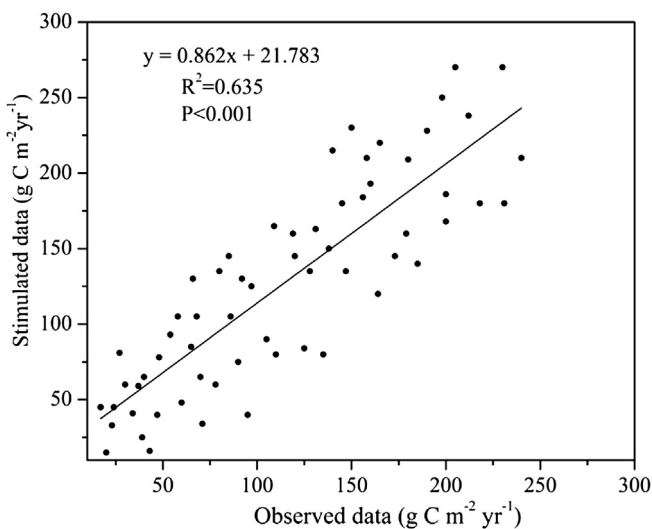


Fig. 2. Plot of estimated NPP using the CASA-model compared with the observed values for the northwest China.

$$V = \frac{1.05r}{\sqrt{1 + (1 + 1.05r/L)^2}} \tag{5}$$

$$L = 3000 + 25t + 0.05t^3 \tag{6}$$

where L is the annual average evapotranspiration (mm), r is annual precipitation (mm), and t is the annual average temperature ($^{\circ}\text{C}$).

2.3.4. Grassland dynamics assessment

The vegetation dynamics measured using NPP is the most intuitive manifestations of land degradation and they reflect the ecological process involved in land degradation. Therefore, NPP was used in this study to assess grassland degradation or restoration. The slope was determined using Ordinary Least Squares regression.

The significance of slope was measured in this study using the statistic F test, following the method proposed by Song et al. (2010). Additionally, the grassland NPP trend was classified into six types according to the significance test (Fig. 4B) and the slope of the NPP (Fig. 4A).

To determine whether the total NPP increased or decreased during the study period, we estimated the change in NPP for each pixel using the following equation:

$$\Delta NPP = (n - 1) \times \text{slope} \tag{7}$$

where $n = 10$ years, representing the study period from 2001 to 2010. This approach is more rational than directly computing the difference between the NPP in 2010 and that in 2001.

2.3.5. Scenario design and quantitative assessment method

The vegetation dynamics measured in terms of NPP is currently used to distinguish the environmental effects of climate change from those of human activities (Wessels et al., 2008; Zheng et al., 2006; Wang et al., 2012). If the relationship between the change in NPP induced by climate change and that induced by human activities are identified, the relative roles of the two factors in grassland degradation can be quantitatively assessed. This quantitative assessment approach is based on the procedure used by Xu et al. (2010). To validate this proposal, we compared the potential vegetation conditions with the actual conditions.

In this study, we defined three kinds of NPP. The first is actual NPP, which is calculated using the CASA model and is used to evaluate grassland dynamics based on the slope of the actual NPP (S_A). A positive S_A indicates grassland restoration, whereas a negative S_A indicates grassland degradation. The second is potential NPP, which represents the change in NPP caused by climate change and potential vegetation conditions, and is estimated using the Thornthwaite memorial model. The third is the loss of NPP because of human activities (LNPP), which equals the difference between potential and actual NPP (i.e., $LNPP = NPP_{\text{potential}} - NPP_{\text{actual}}$) and reflects the effects of human activities on vegetation productivity.

The effect of inter-annual climate changes on grassland vegetation dynamics can be gauged using the slope of potential NPP (S_P), which estimates productivity in the absence of human activities. A positive S_P indicates that the inter-annual climate change during this period is beneficial to grass growth, whereas a negative S_P demonstrates that the inter-annual climate change reduces grass growth.

The effect of human activities on grass growth can be assessed based on the slope of LNPP (S_H). If S_H is negative, that is, the loss of NPP induced by human appropriation decreased during the study period, then, human activities are beneficial to grass growth, which indicates that the grassland restoration was human dominated.

Conversely, a positive S_L indicates that human activities are harmful to grass growth, and human-dominated grassland degradation occurs. Finally, eight scenarios were created based on S_A , S_P , and S_L in this study (Table 1).

Under the situation of grassland restoration ($S_A > 0$), if S_P and S_H are both positive (Scenario 1), grassland restoration is entirely attributed to inter-annual climate change (i.e., the contribution of climate to grassland restoration is 100%), because a positive S_P indicates that the climate is beneficial to grass growth, whereas a positive S_L shows that human activities hinder grass productivity and are harmful to grass growth. If S_P and S_L are both negative (Scenario 2), grassland restoration is attributed entirely to human activities (i.e., the contribution of human activities to grassland restoration is 100%), because a negative S_P indicates that grassland productivity decreased in response to climate, whereas a negative S_L shows that human activities are beneficial to grass growth. If S_P is positive and S_L is negative (Scenario 3), grassland restoration resulted from the positive effects of both climate and human factors, and the individual contribution of each factor to grassland restoration was calculated using the equation shown in Table 1. The contributions of the two factors to grassland degradation were calculated in an analog way.

3. Results

3.1. Current grassland vegetation status

The actual grassland NPP in the study area in 2010 is shown in Fig. 3. The spatial distribution of grassland NPP was clearly heterogeneous. The mean actual grassland NPP was $123.10 \text{ g C m}^{-2} \text{ yr}^{-1}$ in 2010. NPP values higher than $200 \text{ g C m}^{-2} \text{ yr}^{-1}$ were evidently distributed in most regions of the study area, including northeast IM, Tianshan, and Altai Mountains, southeast Tibet, east and south Qinghai, south Gansu, and the middle region of the Hexi Corridor near the Qilian Mountains. These regions accounted for 23% of the total grassland in the study area. In short, these regions with abundant water resources are covered with meadows, as well as alpine and subalpine meadows. Regions with actual NPP values ranging from $100 \text{ g C m}^{-2} \text{ yr}^{-1}$ to $200 \text{ g C m}^{-2} \text{ yr}^{-1}$ were widespread, particularly in the eastern area of the IM and the southwestern Tibetan Plateau, which account for 26.3% of the total grassland area. Actual NPP values ranging from $50 \text{ g C m}^{-2} \text{ yr}^{-1}$ to $100 \text{ g C m}^{-2} \text{ yr}^{-1}$ were widespread across the five big pasture provinces. Regions with actual NPP values less than $50 \text{ g C m}^{-2} \text{ yr}^{-1}$ were found in north Tibet and south Xinjiang along the Kunlun Mountains, which account for 20.4% of the total grassland area. These regions are characterized by desert grasslands. Areas with actual NPP values less than $100 \text{ g C m}^{-2} \text{ yr}^{-1}$ accounted for 50.7% of the total grassland area.

3.2. Changes in grassland productivity

The grassland degradation dynamics based on the slope of the actual NPP are shown in Fig. 4. The overall trend of grassland vegetation tended toward degradation, and the total identified degraded grasslands were 1.65 million km^2 from 2001 to 2010, which accounted for 61.49% of the total grassland area. In comparison, the restored grasslands amounted to 1.03 million km^2 , accounting for 38.51% of the total grassland area (Fig. 4). Furthermore, the slope of the grassland actual NPP (Fig. 4A) and the significance test of the slope (Fig. 4B) both showed that the changes in grasslands were heterogeneous. Moderately degraded grasslands are mainly found in east IM, southeast Tibet, and south Qinghai, as well as scattered in the Tianshan and Altai Mountains. By contrast, moderately restored grasslands were widespread in the five provinces, particularly in Gansu and the Tianshan Mountains. The total actual grassland NPP decreased by 8459.55 Gg C from 2001 to 2010 because the total area of the degraded grasslands (1.65 million km^2 , accounting for 61.49% of the total grassland area) was larger than the restored grasslands area (1.03 million km^2 , equivalent to 38.51% of the total grassland area). Furthermore, the mean actual NPP in the degraded part ($-10.65 \text{ g C m}^{-2} \text{ yr}^{-1}$) was larger than the mean NPP in the restored region ($8.81 \text{ g C m}^{-2} \text{ yr}^{-1}$; Table 2).

The changes in the grasslands in the five provinces varied greatly (Fig. 4), with the largest degraded area in Tibet ($66.97 \times 10^4 \text{ km}^2$), which accounts for 40.59% of the total area of degraded grasslands. Additionally, the five provinces had three different outcomes. First, the percentage of grassland degradation area was larger than the restoration area; this is more common in Tibet (71.02% vs. 28.98%), Xinjiang (58.82% vs. 41.18%), and Qinghai (62.68% vs. 37.32%) (Fig. 5). Second, the percentages of degradation and restoration reached near equilibrium in IM (51% vs. 49%). Third, the grassland restoration area was larger than the degradation area in Gansu (55.2% vs. 44.8%).

3.3. Relative roles of inter-annual climate change and human activities in grassland degradation

The relative roles of inter-annual climate change and human activities in grassland degradation or restoration were assessed based on the methods listed in Table 1. Climate-dominated grassland degradation accounted for only 19.94% of the total grassland degradation area, whereas human-dominated degradation accounted for 65.75%, and the areas where both climate and human factors contributed to degradation accounted for 14.31% (Table 3). The contributions of climate and of human factors to grassland degradation were heterogeneous (Fig. 6). Additionally, climate-dominated degradation was mainly observed in the middle region of Tibet, the Tianshan Mountains, the western IM, and the

Table 1
Eight scenarios for assessing the relative roles of inter-annual climate change and human activities in grassland restoration or degradation.

		S_P	S_L	Relative role of climate change (%)	Relative role of human activities (%)
Grassland restoration ($S_A > 0$)	Scenario 1	>0	>0	100	0
	Scenario 2	<0	<0	0	100
	Scenario 3	>0	<0	$\frac{ \Delta NPP_c }{ \Delta NPP_c + \Delta NPP_L } \times 100\%$	$\frac{ \Delta NPP_L }{ \Delta NPP_c + \Delta NPP_L } \times 100\%$
	Scenario 4	<0	>0		
Grassland degradation ($S_A < 0$)	Scenario 1	<0	<0	100	0
	Scenario 2	>0	>0	0	100
	Scenario 3	<0	>0	$\frac{ \Delta NPP_c }{ \Delta NPP_c + \Delta NPP_L } \times 100\%$	$\frac{ \Delta NPP_L }{ \Delta NPP_c + \Delta NPP_L } \times 100\%$
	Scenario 4	>0	<0		

Note: Scenario1: Climate-induced grassland restoration or degradation; Scenario2: Human-induced grassland restoration or degradation; Scenario3: Grassland restoration or degradation resulted from the interaction of climate change and human activities; Scenario 4: Both climate change and human activities actually benefits the grassland degradation or restoration, but in this methods, restoration or degradation occurred, this judgment is wrong. ΔNPP_C is the total increase or decrease of potential NPP during 2001–2010 can be calculated using Eq. (7), ΔNPP_L is the total increase or decrease of LNPP (difference between potential NPP and actual NPP).

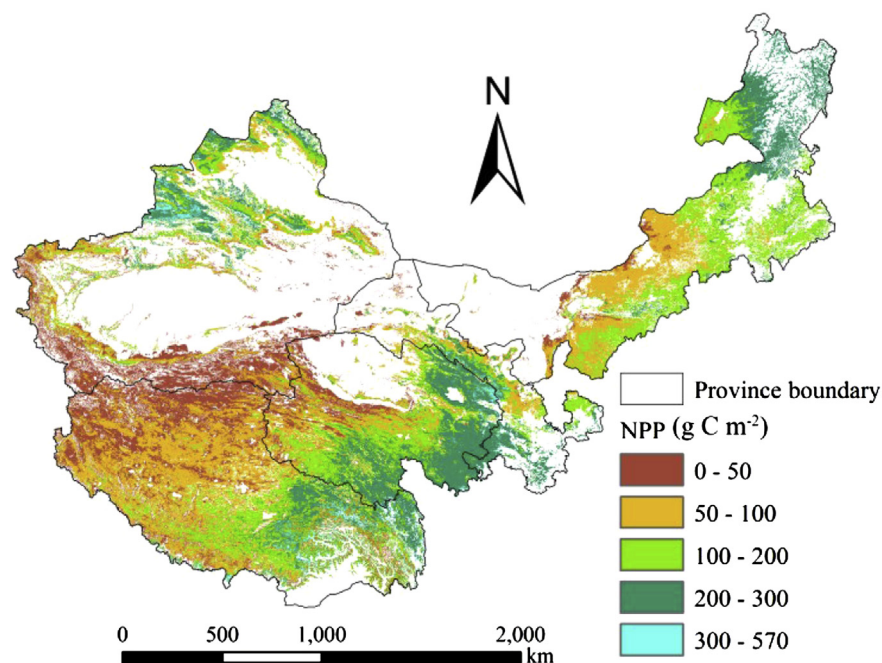


Fig. 3. Spatial distribution of actual grassland NPP across the five provinces in 2010.

eastern Hexi Corridor (Fig. 6A). However, human-dominated degradation was widespread in the study area, especially in Qinghai, Xinjiang, IM, and Tibet (Fig. 6B).

The spatial distribution of the relative roles of climate change and human activities in grassland degradation in the five provinces are shown in Fig. 7A. The effects of human activities on grassland degradation can be observed in all of the five provinces, particularly in Qinghai, where 98.03% of grassland degradation was attributed to human activities compared with only 0.23% induced by climate change; the rest was caused by the combined climate change and human activities (Table 3).

3.4. Relative roles of inter-annual climate change and human activities in grassland restoration

Unlike grassland degradation, the climate-induced grassland restoration area was larger than the human-induced restoration area (56.56% vs. 32.32%), as shown in Fig. 8 and Table 4. Additionally, 11.11% of the total restoration area was attributed to the combined factors. Moreover, climate-induced restoration was widespread in the study area, particularly in Qinghai, west of the Hexi Corridor near the Qilian Mountains, northeast of IM, south of Xinjiang, and northwest of Tibet near the Kunlun Mountains (Fig. 8A). However, human-induced restoration areas were scattered across the southwest of IM, south of Gansu, middle of Tibet, and some regions near the Tianshan Mountains (Fig. 8B).

The relative effects of the two factors on grassland restoration in the five provinces varied greatly in terms of the spatial distribution pattern (Fig. 8) and statistical results (Fig. 7 and Table 4). Three different outcomes were observed in the five provinces. First, the effect of climate on restoration was greater than that of human activity, particularly in Qinghai (94.04% vs. 0.77%), IM (44.84% vs. 38.58%), and Xinjiang (57.94% vs. 30.44%). Second, human-induced restoration areas were larger than climate-induced restoration areas in Gansu (43.07% vs. 39.70%). Third, the contributions of human and climatic factors to grassland restoration were almost equal in Tibet (46.63% vs. 45.67%).

4. Discussion

4.1. Quantitative assessment methods for grassland degradation

The monitoring and assessment of grassland degradation traditionally depend on field surveys (Li, 1997), which is inefficient. The results obtained through this traditional method are unreliable because grasslands usually cover large areas (Asrar et al., 1986). Assessing grassland degradation through remote sensing is much more efficient (Alfredo et al., 2002; Lu et al., 2007). Although previous studies have assessed grassland degradation using satellite imagery (Shi et al., 1999; Liu et al., 2004), these studies merely classified the degree of grassland degradation and constructed spatial distribution maps. Quantitative assessments of the factors that determine grassland degradation and analyses of the degradation dynamics at a large spatiotemporal scale are few in China. Although the quantitative assessment of the relative roles of climate and human factors in grassland degradation is definitely challenging, this assessment is essential to determining the main cause of grassland degradation.

Grassland degradation refers to the overall reduction in grassland productivity induced by human activities and the natural environment. This degradation is reflected by reduced grass coverage, grass density, and biological diversity or by increased unpalatable grass species and toxic weeds, and even soil erosion (Li, 1997; Liu et al., 2004). Therefore, in the current study, NPP was selected as an indicator for monitoring grassland degradation because it reflects grassland degradation, and it is easily estimated using remote sensing data. Additionally, NPP can be used as an intuitive vegetation dynamic indicator for distinguishing the effects of climate change from human activities on desertification (Zheng et al., 2006; Xu et al., 2010). In this study, we designed a method for distinguishing the effects of inter-annual climate change on grassland degradation from human activities based on three kinds of NPP. We calculated the actual NPP using the CASA model, which is a light use efficiency model. The actual NPP reflects the effects of human and climate factors on grassland productivity and the slope

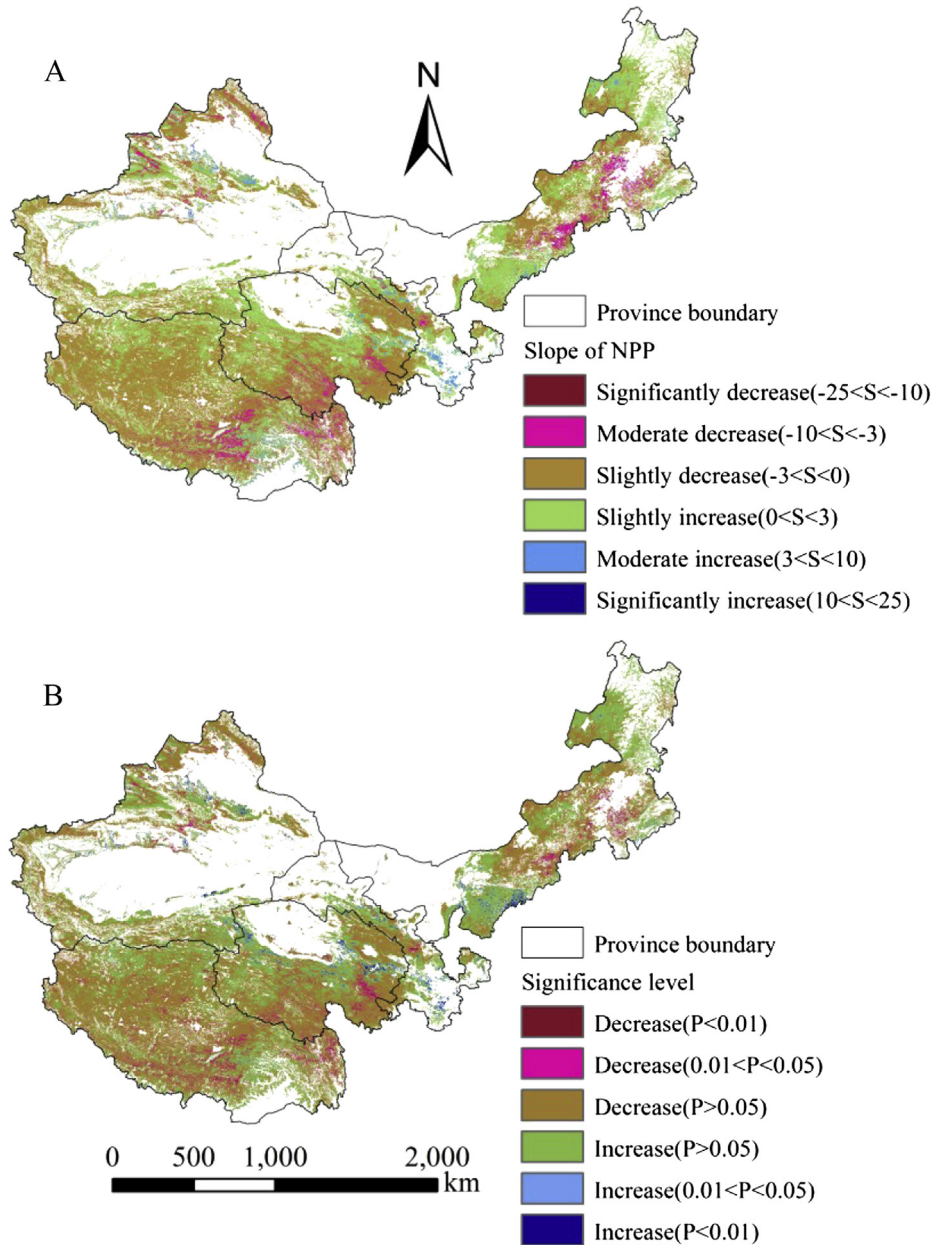


Fig. 4. Grassland vegetation dynamics based on the slope of the actual NPP (A); and the significance test of the slope of the actual NPP (B) from 2001 to 2010.

of actual NPP was therefore used to determine grassland degradation and restoration dynamics. Potential NPP was estimated using the Thornthwaite memorial model, which is a climate-productivity model. The potential NPP is an indicator for measuring the effects of inter-annual variations in climate on grassland productivity. The loss of NPP because of human activities was the difference between potential NPP and actual NPP, which reflects the effects of human activities on vegetation productivity.

4.2. Effects of inter-annual variations in climate on grassland degradation

Previous studies have shown that land degradation is caused by feedback interaction between climate change and human activities. In this process, climate change is an intrinsic controlling driving force, whereas human activities is an external driving force that can intensify or alleviate the effects of climate change to some extent

(Wang et al., 2006b; Zheng et al., 2006). Our findings show that inter-annual climate change dominated grassland restoration, contributing up to 56.56%, whereas the effects of human activities-dominated grassland degradation exceeded 65%. This result is consistent with those by Zheng et al. (2006) who found that climate change is beneficial to vegetation growth and desertification reversion in the Otindag sandy land in the past 40 years. Meanwhile, Zhang et al. (2011) concluded that climate change contributed 49.7% of the vegetation restoration compared with only 16.9% caused by human activities. Recent studies have suggested that the climate in northwest China has changed from warm-dry to warm-wet since the late 1980s, and some regions have become significant conversion regions, including north Xinjiang, the Tianshan Mountains, west Tarim Basin, and the Qilian Mountains (Shi et al., 2007; Wang et al., 2007). Wang et al. (2004b) found that although precipitation across China has slightly declined since 1951 to 2000, the precipitation in northwest China has significantly increased since

Table 2

Grassland vegetation dynamics in terms of area (million km²), mean NPP (g C m⁻²), and total NPP (Gg C = 10⁹ g C).

	Area	Mean NPP variation	Total NPP
Restoration region	1.03	8.81	9107.73
Degradation region	1.65	-10.65	-17567.28
Total study area	2.68	-3.15	-8459.55

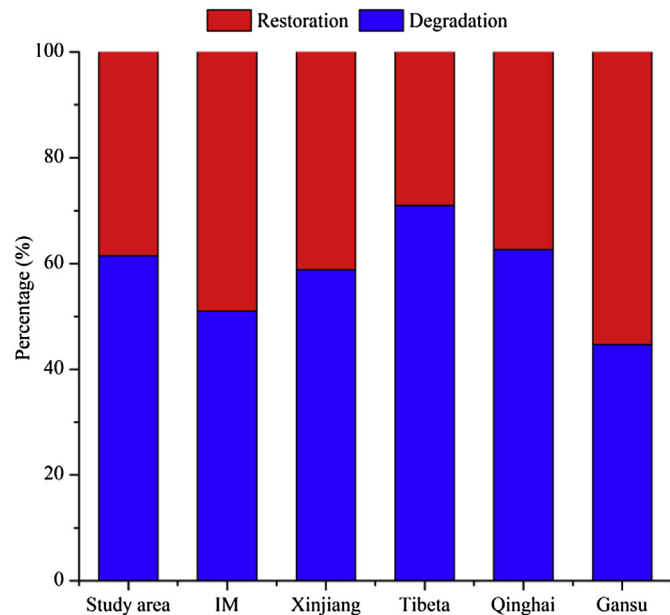


Fig. 5. Area percentages of grassland degradation and restoration in the five provinces. IM is the abbreviation of Inner Mongolia.

1986. [Zhai et al. \(2005\)](#) analyzed the change in precipitation in China from 1950 to 2008 and found that precipitation increased significantly in the Tianshan Mountains, southeastern Tibet, and the western Tarim Basin. [Qi et al. \(2012\)](#) also concluded that the climate in Xinjiang exhibited a wet trend from 1940 to 2008. Meanwhile, [Sun et al. \(2013\)](#) found that the annual temperature increased by 0.45 °C/10 yr and the precipitation increased by 43.2 mm/10 yr from 1960 to 2002 in the Tibetan Plateau, but western Tibet became warm and dry. In this study, we found that the annual precipitation increased from 1981 to 2010 in most regions in northwestern China ([Fig. 9](#)), which is consistent with the results of previous studies. Meanwhile, the actual grassland NPP increased in the aforementioned selected regions ([Fig. 4](#)) because the increased precipitation is beneficial to the growth of vegetation, particularly in dry areas ([Herrmann et al., 2005](#)).

In this paper, we show that the inter-annual climate change promote grassland restoration; however, this effect varies greatly across the study area. Moreover, the contribution of climate change is greater than that of human activities, even in Qinghai, Xinjiang, and IM. This finding is especially highlighted in Qinghai, where 94.04% of the grassland restoration was induced by climate change. However, in Tibet and Gansu, the contribution of climate change to grassland restoration is less than that of human activities because precipitation decreased in most parts of Tibet from 1981 to 2010, whereas the temperature increased. These findings are consistent with the study by [Cui and Graf \(2009\)](#), which concluded that warmer and drier climates are harmful to vegetation growth.

4.3. Effects of human intervention on grassland degradation

The climate change in recent decades cannot solely account for the severe land degradation in China; human activities are a pervasive catalyst for land degradation because land use covers changes and management measures largely govern the sustainability of a given land ([Foley et al., 2005](#)). Human activities, such as overgrazing, conversion of grasslands into farmlands, overcutting, and overexploitation of water resources lead to vegetation degradation. This study has confirmed that over 65% of grassland degradation is caused by human activities, and only 19.94% is induced by inter-annual climatic change. Furthermore, the contribution of human activities to grassland degradation is greater than that of climate change in all the five provinces, especially in Qinghai where 98.03% of the grassland degradation was caused by human activities. These findings are consistent with those of recent studies ([Wang et al., 2006b, 2012; Zhang et al., 2011](#)), which concluded that human activities are the main factors in land degradation of China.

In the recent decades, the Chinese government has implemented several ecological restoration programs to control grassland degradation, such as the Grain to Green Program since 1999 and the Return Grazing to Grass Program since 2003. Both programs focus on alleviating grazing pressure in degraded natural grasslands mainly through fenced enclosure and rotational grazing. In this study, human activities also promoted grassland restoration in Tibet and Gansu, contributing 46.63% and 43.07% to grassland restoration, respectively.

This study show that the contribution of human activities to grassland degradation varied across the five provinces, which is mainly due to the interaction of climate characteristic and socio-economic conditions. A previous research on land degradation (e.g. [Zhang et al., 2011](#)) showed that humans induced land degradation whereas climate induced vegetation restoration in the Shiyanghe River Basin in Gansu Province from 1999 to 2006. [Xu et al. \(2010\)](#) found that climate induced the expansion of desertification in 1980s, whereas humans induced desertification reversal in the

Table 3

Area (10⁴ km²) and percentage (%) of grassland degradation caused by climate changes, human activities, and the combination of these two factors.

		Climate-induced	Human-induced	Two factors-induced	Error
Total study area	Area	32.91	108.51	23.62	0.0002
	Percentage	19.94	65.75	14.31	0.00
Inner Mongolia	Area	4.51	17.73	5.68	0.50
	Percentage	16.16	63.49	20.35	0.00
Xinjiang	Area	6.09	21.68	3.74	0.00003
	Percentage	19.31	68.82	11.87	0.00
Tibet	Area	20.40	33.93	12.64	0.0002
	Percentage	30.45	50.67	18.88	0.00
Qinghai	Area	0.07	3.15	0.56	0.00003
	Percentage	0.23	98.03	1.74	0.00
Gansu	Area	1.84	3.67	0.99	0.00
	Percentage	28.35	56.43	15.22	0.00

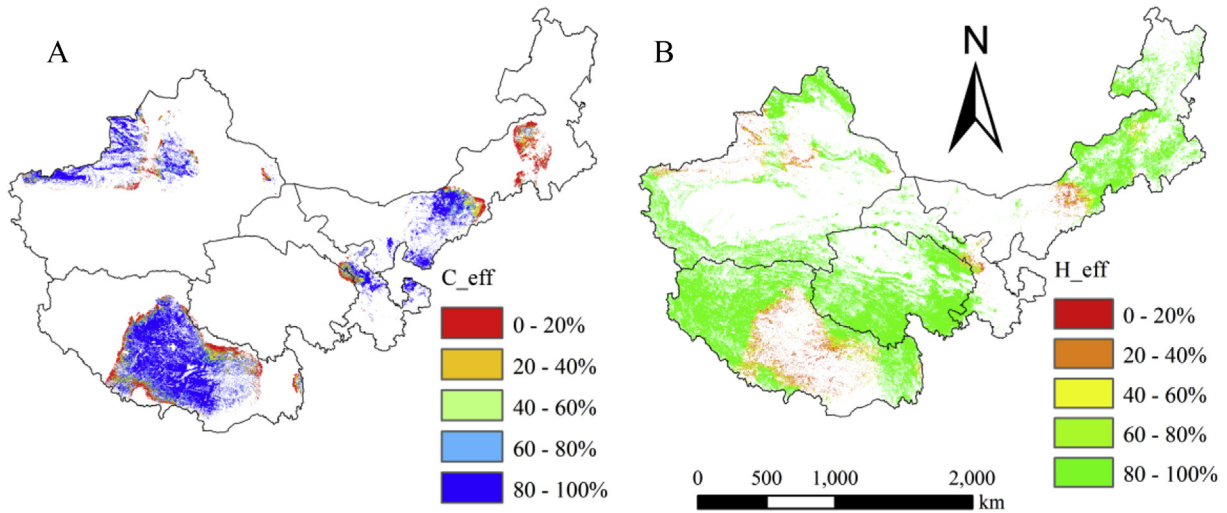


Fig. 6. Proportion of the relative roles of (A) inter-annual climate change and (B) human activities in grassland degradation. C_eff denotes climate-induced grassland degradation and H_eff denotes human-induced grassland degradation.

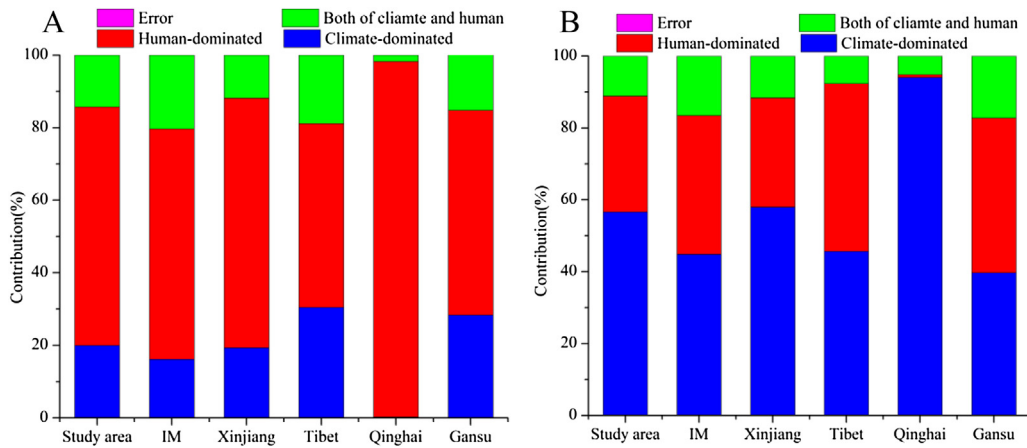


Fig. 7. Contributions of inter-annual climate change, human activities, and the combination of these two factors to grassland degradation (A); and grassland restoration (B). IM is the abbreviation of Inner Mongolia.

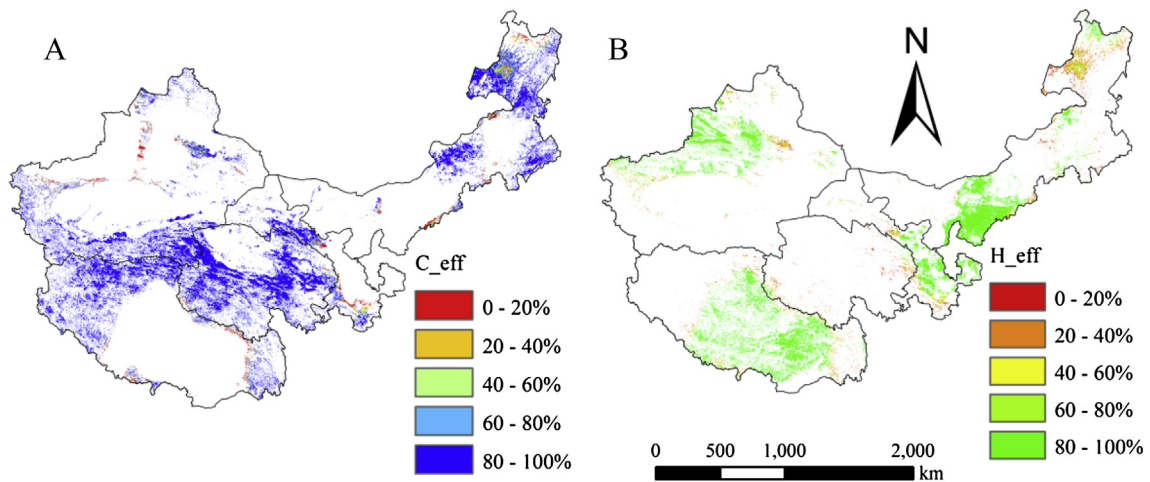


Fig. 8. Proportion of the relative roles of (A) inter-annual climate change and (B) human activities in grassland restoration. C_eff denotes climate-induced grassland restoration and H_eff denotes human-induced grassland restoration.

Table 4Area (10^4 km^2) and percentage (%) of grassland restoration caused by climate change, human activities, and the combination of these two factors.

		Climate-dominant	Human-dominant	Two factors-induced	Error
Total study area	Area	58.47	33.41	11.49	0.0006
	Percentage	56.56	32.32	11.12	0.00
Inner Mongolia	Area	12.03	10.35	4.45	0.00003
	Percentage	44.84	38.58	16.58	0.00
Xinjiang	Area	12.78	6.71	2.56	0.00008
	Percentage	57.94	30.44	11.62	0.00
Tibet	Area	12.48	12.75	2.10	0.0004
	Percentage	45.67	46.63	7.69	0.00
Qinghai	Area	17.99	0.15	1.0	0.0002
	Percentage	94.04	0.77	5.19	0.00
Gansu	Area	3.19	3.46	1.38	0.00003
	Percentage	39.70	43.07	17.23	0.00

Ordos of IM in 1990s. This reversal occurred because desertification control and management have been emphasized because of the implementation of ecological restoration programs since the 1990s (Wu, 2001). Therefore, these ecological restoration programs should be enhanced to protect grassland resources and to achieve sustainable development.

The results of the quantitative assessment show that the assessment incorporated errors, albeit very small and near zero (Tables 3 and 4). These errors may be due to the following conditions: The interpolation accuracy of climate data and the uncertainty associated with the procedure for converting various source datasets to 500 m resolution may have led to errors. Moreover, the regions that experienced land use and cover change (LUCC) or vegetation succession accompanied by increased NPP may have actually undergone land degradation. This land degradation could have resulted in errors during the analysis. In further studies, we will enhance the accuracy of datasets and incorporate LUCC to reduce errors. Although some errors were introduced into our assessment, our proposed method for the quantitative assessment of grassland degradation is applicable to land degradation assessment in other regions.

Two structurally different models were used for estimation of actual and potential NPP, which has a potentially important impact on the estimated difference between the two models. Finally, our results are subject to inherent differences between the two different modeling approaches used to estimate actual and potential NPP. The sensitivity of the attribution to climatic and human causes of degradation and restoration should be evaluated with further multi model comparison studies.

5. Conclusions

We used actual grassland NPP to evaluate grassland dynamics. The trends in actual NPP, potential NPP, and LNPP were used to deconstruct the relative roles of climate change and human activities in grassland degradation. The mean actual grassland NPP in 2010 was approximately $123 \text{ g C m}^{-2} \text{ yr}^{-1}$ and showed obvious spatial heterogeneity. During the study period, 61.49% of the total grassland area exhibited degradation, and the total actual NPP of grasslands decreased by 8459.55 Gg C. In general, inter-annual climate change induced grassland restoration from 2001 to 2010, whereas human activities induced grassland degradation.

The relative roles of climate change and human activities in grassland degradation varied greatly in the five provinces. The contribution of human activities to grassland degradation was greater than that of climate change, which is common in all five provinces, especially in Qinghai where 98.03% of the degradation was induced by human activities. Three different outcomes were observed in terms of grassland restoration. First, the effect of climate to grassland restoration was greater than that of human activities, even in Qinghai, IM, and Xinjiang. Second, the effect of human activities on grassland restoration was greater than that of climate in Gansu. Third, the contributions of human activities and climate factors to grassland restoration were almost equal in Tibet. Therefore, the management measures and policies for protecting grassland resources should be improved to control grassland degradation, as well as decrease dust storm and increase carbon sequestration in grassland ecosystems.

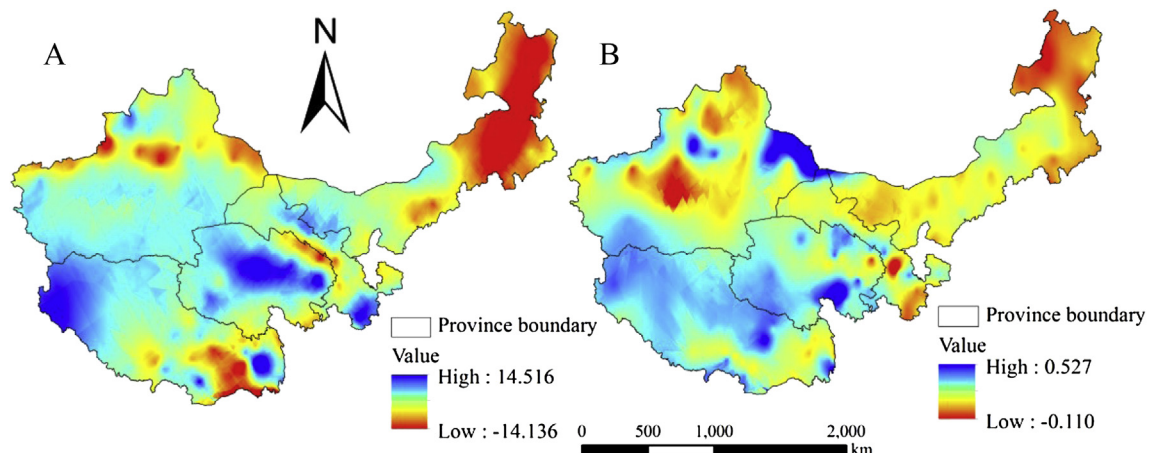


Fig. 9. Climate change trend from 1981 to 2010 in relation to (A) annual precipitation and (B) annual temperature.

Acknowledgments

We are grateful to the chief editor and anonymous reviewers for illuminating comments. This work was supported by National Basic Research Program of China (2010CB950702), the Asia–Pacific Network (ARCP-2013-16NMY-Li), and National Natural Science Foundation of China (41271361), the Public Sector Linkages Program supported by Australian Agency for International Development (64828). We also thank the China Meteorological Data Sharing Service System for granting us access to climate datasets.

References

- Alfredo, C.D., Emilio, C.W., Ana, C., 2002. Satellite remote sensing analysis to monitor desertification processes in the crop-rangeland boundary of Argentina. *J. Arid Environ.* 52, 121–133.
- Asrar, G., Weiser, R.L., Johnson, D.E., Kanemasu, E.T., Killeen, J.M., 1986. Distinguishing among tall grass prairie cover types from measurements of multi-spectral reflectance. *Remote Sens. Environ.* 19, 159–169.
- Chase, T.N., Pielke Sr, R.A., Knapp, J.A., Kittel, T.G.F., Eastman, J.L., 2000. A comparison of regional trends in 1979–1997 depth-averaged tropospheric temperatures. *Int. J. Climatol.* 20, 503–518.
- Chen, S.B., Liu, Y.F., Axel, T., 2006. Climatic change on the Tibetan Plateau: potential evapotranspiration trends from 1961–2000. *Clim. Change* 76, 291–319.
- Chen, Z., Wang, S., 2000. Typical Grassland Ecosystem in China. Science Press, Beijing.
- Conant, R.T., Paustian, K., Elliott, E.T., 2001. Grassland management and conversion into grassland: effects on soil carbon. *Ecol. Appl.* 11, 343–355.
- Cui, X., Graf, H.F., 2009. Recent land cover changes on the Tibetan Plateau: a review. *Clim. Change* 94, 47–61.
- Evans, J., Geerken, R., 2004. Discrimination between climate and human-induced dryland degradation. *J. Arid Environ.* 57, 535–554.
- Fang, J.Y., Liu, G.H., Xu, S.L., 1996. Carbon storage in terrestrial ecosystem of China. In: Wang, G.C., Wen, Y.P. (Eds.), *The Measurement of Greenhouse Gas and Their Release and Related Processes*. China Environmental Science Press, Beijing, pp. 391–397.
- Field, C.B., Randerson, J.T., Malmström, C.M., 1995. Global net primary production: combining ecology and remote sensing. *Remote Sens. Environ.* 51, 74–88.
- Foley, J.A., DeFries, R., Asner, G.P., Barford, C., Bonan, G., Carpenter, S.R., Chapin, F.S., Coe, M.T., Daily, G.C., Gibbs, H.K., Helkowski, J.H., Holloway, T., Howard, E.A., Kucharik, C.J., Monfreda, C., Patz, J.A., Prentice, I.C., Ramankutty, N., Snyder, P.K., 2005. Global consequences of land use. *Science* 309, 570–574.
- GLC, 2003. Global land cover classification for the year 2000. <http://www-gem.jrc.it/glc2000/>.
- Haberl, H., Krausmann, F., Erb, K.H., Schulz, N.B., 2002. Human appropriation of net primary production. *Science* 296, 1968–1969.
- Hanafi, A., Jauffret, S., 2008. Are long-term vegetation dynamics useful in monitoring and assessing desertification processes in the arid steppe, southern Tunisia. *J. Arid Environ.* 72, 557–572.
- Herrmann, S.M., Anyamba, A., Tucker, C.J., 2005. Recent trends in vegetation dynamics in the African Sahel and their relationship to climate. *Glob. Environ. Chang.* 15, 394–404.
- Huddleston, B., de Salvo, E.A.P., Zanetti, M., Blaise, M., Bel, J., Franceschini, G., D'Ostiani, L.F., 2003. Towards a GIS-based Analysis of Mountain Environments and Populations. Environment and Natural Resources working paper No. 10. Food and Agricultural Organisation, Rome.
- Jiang, G.M., Han, X.G., Wu, J.G., 2006. Restoration and management of the Inner Mongolia grassland require a sustainable strategy. *Ambio* 35, 269–270.
- Kang, L., Han, X., Zhang, Z., Sun, O.J., 2007. Grassland ecosystems in China: review of current knowledge and research advancement. *Philos. Trans. R. Soc. B-Biol. Sci.* 362, 997–1008.
- Li, B., 1997. The degradation of grassland in North China and its countermeasure. *Agric. Sci. Sin.* 30, 1–10.
- Li, S., 1993. Agroclimatic resources and agricultural distribution patterns. In: Cheng, C. (Ed.), *Climate and Agriculture in China*. China Meteorological Press, Beijing, pp. 30–69.
- Lieth, H., Box, E., 1972. Evapotranspiration and primary productivity: C.W. Thornthwaite memorial model. *Publ. Climatol.* 25, 37–46.
- Lieth, H., 1975. Modeling the primary production of the world. In: Lieth, H., Whittaker, R.H. (Eds.), *Primary Productivity of the Biosphere*. Springer, Berlin, pp. 237–283.
- Liu, Y., Zha, Y., Gao, J., Ni, S., 2004. Assessment of grassland degradation near Lake Qinghai, West China, using Landsat TM and in situ reflectance spectra data. *Int. J. Remote Sens.* 25, 4177–4189.
- Lu, D., Batistella, M., Mause, P., Moran, E., 2007. Mapping and monitoring land degradation risks in the Western Brazilian Amazon using multitemporal Landsat TM/ETM+ images. *Land Degrad. Dev.* 18, 41–54.
- Nan, Z., 2005. The grassland farming system and sustainable agricultural development in China. *Grassl. Sci.* 51, 15–19.
- Ni, J., 2002. Carbon storage in grasslands of China. *J. Arid Environ.* 50, 205–218.
- Potter, C.S., Randerson, J.T., Matson, P.A., Vitousek, H.A., Mooney, H.A., Klooster, S.A., 1993. Terrestrial ecosystem production—a process model-based on global satellite and surface data. *Glob. Biogeochem. Cycle* 7, 811–841.
- Prince, S.D., Colstoun, D., Brown, E., Kravitz, L.L., 2004. Evidence from rain-use efficiencies does not indicate extensive Sahelian desertification. *Glob. Change Biol.* 4, 359–374.
- Qi, J.G., Chen, J.Q., Wan, S.Q., Ai, L.K., 2012. Understanding the coupled natural and human systems in dryland East Asia. *Environ. Res. Lett.* 7, 015202.
- Rojstaczer, S., Sterling, S.M., Moore, N.J., 2001. Human appropriation of photosynthesis products. *Science* 294, 2549–2552.
- Schimel, D.S., 1995. Terrestrial biogeochemical cycles: global estimates with remote sensing. *Remote Sens. Environ.* 51, 49–56.
- Scurlock, J., Hall, D.O., 1998. The global carbon sink: a grassland perspective. *Glob. Change Biol.* 4, 229–233.
- Shi, D., Qiao, A., Sai, W., Hon, X., Hodgson, N., 1999. Applied research on use of remote sensing to study alpine grassland resource and degradation. *Grassl. Qinghai* 8, 1–6.
- Shi, Y.F., Shen, Y.P., Kang, E., Li, D.L., Ding, Y.J., Zhang, G.W., Hu, R.J., 2007. Recent and future climate change in northwest China. *Clim. Change* 80, 379–393.
- Song, Y., Ma, M.G., Veroustraete, F., 2010. Comparison and conversion of AVHRR GIMMS and SPOT VEGETATION NVDI data in China. *Int. J. Remote Sens.* 31, 2377–2392.
- Sun, J., Cheng, G.W., Li, W.P., Sha, Y.K., Yang, Y.C., 2013. On the variation of ndvi with the principal climatic elements in the Tibetan plateau. *Remote Sens.* 5, 1894–1911.
- Symeonakis, E., Drake, N., 2004. Monitoring desertification and land degradation over sub-Saharan Africa. *Int. J. Remote Sens.* 25, 573–592.
- Turner II, B.L., Villar, S.C., Foster, D., Geoghegan, J., Keys, E., Klepeis, P., Lawrence, D., Mendoza, P.M., Manson, S., Ogneva-Himmelberger, Y., 2001. Deforestation in the southern Yucatan peninsular region: an integrative approach. *For. Ecol. Manag.* 154, 353–370.
- Ueno, K., Fujii, H., Yamada, H., Liu, L.P., 2001. Weak and frequent monsoon precipitation over the Tibetan Plateau. *J. Meteorol. Soc. Jpn.* 79, 419–434.
- Veron, S.R., Paruelo, J.M., Oesterheld, M., 2006. Assessing desertification. *J. Arid Environ.* 66, 751–763.
- Wang, S., Wang, Y.M., Wang, R.Y., Zhang, P., Wang, J.S., Wang, H.L., 2007. Review of climate change and water resource research in Qilian Mountain region in recent ten years. *Arid Meteorol.* 23, 82–87.
- Wang, S.P., Wilkes, A., Zhang, Z.C., Chang, X.F., Lang, R., Wang, Y.F., Niu, H.S., 2011. Management and land use change effects on soil carbon in northern China's grasslands: a synthesis. *Agr. Ecosyst. Environ.* 142, 329–340.
- Wang, T., Sun, J.G., Han, H., Yan, C.Z., 2012. The relative role of climate change and human activities in the desertification process in Yulin region of northwest China. *Environ. Monit. Assess.* 184, 7165–7173.
- Wang, W.Y., Wang, Q.J., Wang, H.C., 2006a. The effect of land management on plant community composition, species diversity, and productivity of alpine Kobersia steppe meadow. *Ecol. Res.* 21, 181–187.
- Wang, X.M., Chen, F.H., Dong, Z.B., 2006b. The relative role of climatic and human factors in desertification in semiarid China. *Glob. Environ. Change* 16, 48–57.
- Wang, X.M., Dong, Z.B., Zhang, J.W., Liu, L.C., 2004a. Modern dust storms in China: an overview. *J. Arid Environ.* 58, 559–574.
- Wang, Z.Y., Ding, Y.H., He, J.H., Yu, J., 2004b. An updating analysis of the climate change in China in recent 50 years. *Acta Meteorol. Sin.* 62, 228–236.
- Wessels, K.J., Prince, S.D., Malherbe, J., Small, J., Frost, P.E., VanZyl, D., 2007. Can human-induced land degradation be distinguished from the effects of rainfall variability? A case study in South Africa. *J. Arid Environ.* 68, 271–297.
- Wessels, K.J., Prince, S.D., Reshef, I., 2008. Mapping land degradation by comparison of vegetation production to spatially derived estimates of potential production. *J. Arid Environ.* 72, 1940–1949.
- Wu, W., 2001. Study on process of desertification in Mu Us sandy land for last 50 years, China. *J. Desert Res.* 21, 164–169.
- Xin, H., 2008. A green fervor sweeps the Qinghai-Tibetan Plateau. *Science* 321, 633–635.
- Xu, D.Y., Kang, X.W., Zhuang, D.F., Pan, J.J., 2010. Multi-scale quantitative assessment of the relative roles of climate change and human activities in desertification—a case study of the Ordos Plateau, China. *J. Arid Environ.* 74, 498–507.
- Yang, R.Y., 2002. Studies on current situation of grassland degradation and sustainable development in western China. *Pratacul. Sci.* 19, 23–27.
- Yu, D.Y., Shi, P.J., Han, G.Y., Zhu, W.Q., Du, S.Q., Xun, B., 2011. Forest ecosystem restoration due to a national conservation plan in China. *Ecol. Eng.* 37, 1387–1397.
- Zhai, P.M., Zhang, X.B., Wan, H., Pan, X.H., 2005. Trends in total precipitation and frequency of daily precipitation extremes over China. *J. Clim.* 18, 1096–1108.
- Zhang, C.X., Wang, X.M., Li, J.C., Hua, T., 2011. Roles of climate changes and human interventions in land degradation: a case study by net primary productivity analysis in China's Shiyanghe Basin. *Environ. Earth Sci.* 64, 2183–2193.
- Zheng, Y.R., Xie, Z.X., Robert, C., Jiang, L.H., Shimizu, H., 2006. Did climate drive ecosystem change and induce desertification in Otindag sandy land, China over the past 40 years? *J. Arid Environ.* 64, 523–541.
- Zhu, W., Pan, Y., He, H., Yu, D., Hu, H., 2006. Simulation of maximum light use efficiency for some typical vegetation types in China. *Chin. Sci. Bull.* 51, 457–463.